Determination of e/m, mc^2, and the Relations Among Momentum, Velocity, and Energy of Relativistic Electrons

Edwin Ng*
MIT Department of Physics
(Dated: November 16, 2011)

Using a spherical electromagnet, a velocity selector, and an Si diode detector, we measure the velocities and kinetic energies of relativistic ($\sim 0.8c$) electrons emitted from a beta decay source. We compare the data to classical and relativistic predictions, and use the relativistic model to obtain estimates on the electron charge-to-mass ratio and (independently) the electron mass. We determine $e/m = (1.55 \pm 0.008_{\text{rand.}} \pm 0.31_{\text{syst.}}) \times 10^{11}\,\text{C/kg}$ and $mc^2 = (612 \pm 5_{\text{rand.}} \pm 170_{\text{syst.}})\,\text{keV}$.

I. INTRODUCTION AND THEORY

According to the theory of special relativity proposed by Albert Einstein in 1905, the postulate that the speed of light c is a universal constant, together with the principle of relativity, requires particles moving at velocities close to c to exhibit non-classical relationships between their velocity, momentum, and kinetic energy.

In Newtonian mechanics, the velocity v, momentum p, and kinetic energy K of a particle with mass m are related by

$$p = mv \tag{1}$$

and

$$K = \frac{1}{2}mv^2 = \frac{p^2}{2m}. \tag{2}$$

However, in special relativity, we are instead given

$$p = m\gamma v, \tag{3}$$

where $\gamma = 1/\sqrt{1-\beta^2}$ for $\beta = v/c$. Furthermore, the energy E of the particle is made up of $E = K + mc^2$, where mc^2 is the rest mass energy, and E is related to p by the relativistic dispersion equation

$$E^2 = p^2c^2 + m^2c^4.$$

Using the dispersion relation and Eq. 3, we obtain

$$K = mc^2\,(\gamma - 1) \simeq pc, \tag{4}$$

where the last approximation holds in the ultrarelativistic limit of $p \gg mc$.[1]

In this experiment, electrons are accelerated by a magnetic field B in a circular path of radius ρ. The Lorentz force yields the equation of motion

$$\frac{\mathrm{d}p}{\mathrm{d}t} = \left(\frac{v}{\rho}\right)p = \frac{evB}{c},$$

so p and B are related by

$$p = \left(\frac{e\rho}{c}\right)B. \tag{5}$$

At the end of the path, the electrons go through a velocity selector. The electric field E across the selector plates necessary to cancel the Lorentz force and have electrons pass through satisfies $eE - evB/c = 0$, or

$$\beta = E/B \tag{6}$$

Therefore, B determines the momentum and measurement of E for a given B yields the velocity.

II. EXPERIMENTAL SETUP

II.1. Apparatus Details

The experimental setup is shown schematically in Fig. 1 below, including typical electron trajectories.

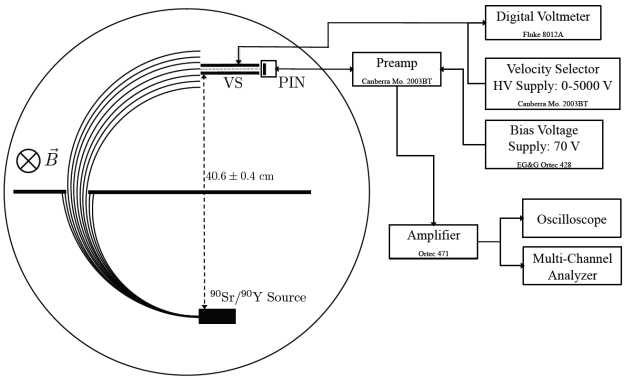

FIG. 1. A schematic of the apparatus. The velocity selector is labelled VS, and the diode detetor PIN. Adapted from [2].

The main apparatus is located inside a spherical electromagnet, shown above with a circle. The top hemisphere of the magnet can be lifted by a block and tackle to reveal the vacuum chamber ($\sim 10^{-5}$ torr) in the lower half. The magnet itself consists of a stack of circular coils connected in series. Current is provided by a Sorenson power supply delivering up to 5.5 A and 200 V.

The ^{90}Sr/^{90}Y source decays by beta emission, with electrons up to 2.27 MeV. These electrons are accelerated into helical paths by the magnetic field, and a set of baffles at the 90° position restricts the electrons to a circular stream towards a Bertran 7.5kV velocity selector.

* ngedwin@mit.edu

The source and the selector are located along the diameter of the magnet, separated by (40.6 ± 0.4) cm. The selector consists of two parallel aluminum blocks separated by a distance (0.180 ± 0.003) cm, with a length of 10 cm. The selector is powered by a Canberra high-voltage power supply capable of delivering up to 5000 V.

After passing through the selector, the electrons hit the Hamamatsu PIN Si diode detector. The detector is biased with a battery voltage source at 67.5 V, and the signal is sent through a Canberra preamp, an Ortec amplifier, and then into the multi-channel analyzer (MCA), which bins the data in 2048 channels.

To measure the magnetic field, we use an RFL Hall effect gaussmeter, which is zeroed each lab session with calibration magnets and placed in the center of the magnet on top of the vacuum chamber. It is held in place by a plastic block and oriented horizontally so as to obtain a maximum field measurement.

Despite a conventional cooling fan, the resistance in the coils gradually changes due to heating by high currents. For fields up to 120 G ($\sim$ 5 A), this effect is alleviated by setting the power supply to current limit, leading to a time-variation in B for a typical 300 s acquisition of only about 0.2 G. However, above 120 G, the power supply is on voltage limit and B varies by approximately 2 G over a typical aquisition. Spatial non-uniformities in the magnetic field are also present, and testing the field at various points around the trajectory of the electrons, we find a deviation of about 1 G. In summary, all our field measurements have an error of 0.5 G except for the highest, centered at 124 G with an error of 1.5 G.

II.2. MCA Calibration

In order to use the MCA to obtain kinetic energy data, we need to determine the gain due to the preamp and amplifier. We use a ^{133}Ba calibration source, which emits gamma rays with known energies.[3]

The ^{133}Ba source is placed next to the PIN diode and left to acquire on the MCA overnight with the magnetic field off. The resulting spectrum is shown in Fig. 2.

The notable features of the spectrum are 1) the 31 keV electron-capture K-shell x-ray peak, 2) the photopeaks of ^{133}Ba, and 3) the associated Compton edges due to scattering in the detector, with energy $2E^2/(mc^2 + 2E)$. To determine the relationship between energies at the detector and the MCA channel numbers, we do a linear fit to the channel numbers of the identified features against their published energy values, by

$$T = \alpha n + \varepsilon, \tag{7}$$

where α is the amplification ratio, and ε is some possible offset at channel 0.

We restrict our attention to the peaks, since they can be identified with a much better precision (approx. ± 3 channels), and the five photopeaks already provide an excellent fit. We find $\alpha = (0.4546 \pm 0.0014)$ keV/channel and $\varepsilon = (-0.2 \pm 1.7)$ (i.e., no offset).

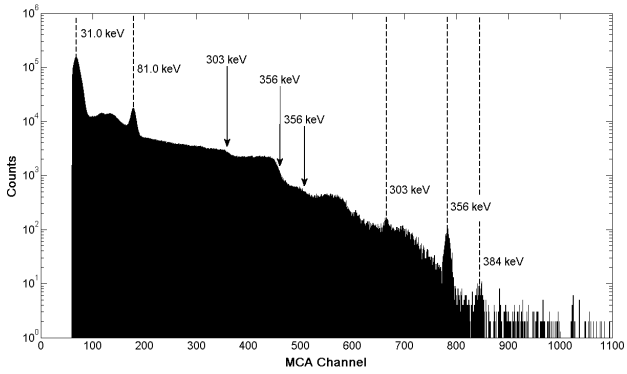

FIG. 2. The MCA spectrum of ^{133}Ba, with counts on log scale. Dotted lines mark the identified peaks, labelled by its energy T as given in [3]. Arrows mark identified Compton edges, also labelled by their associated T.

III. PROCEDURE AND DATA

III.1. Measurements of Velocity

According to Eq. 6, we can determine the electron velocity for each B by measuring the voltage V_0 on the selector such that these electrons pass through. But because there is an inevitable spread in the velocities, we observe appreciable electron counts throughout a range on the order of 1 kV. Thus, to determine V_0, we acquire counts for at least five voltages in this range, and we fit the variation in count rates to a Gaussian model in order to find the voltage with maximum signal, which we identify with V_0.

For an acquisition time T, total count N, and trial voltage V, we compute the count rate $\mu = N/T \pm \sqrt{N}/T$. The variation of μ with V is fit to a Gaussian model, and the mean of the Gaussian is identified with V_0, with an error given by the error of the fit. Since the background is relatively uniform throughout the values of B and V, we include it in our analysis. These results are summarized below in Table I.

TABLE I. Determinations of V_0 and E by Gaussian fit. We use $E = V_0/d$, where $d = (0.180 \pm 0.003)$ cm is the separation distance of the selector plates.

B Field (G)	Voltage V_0 (kV)	E Field (G)
70	2.30 ± 0.02	42.6 ± 0.4
75	2.63 ± 0.02	48.8 ± 0.4
80	2.83 ± 0.03	52.4 ± 0.5
85	3.15 ± 0.02	58.3 ± 0.4
90	3.35 ± 0.02	62.2 ± 0.5
95	3.63 ± 0.02	67.3 ± 0.4
100	3.92 ± 0.02	72.6 ± 0.3
105	4.18 ± 0.02	77.5 ± 0.4
110	4.41 ± 0.03	81.8 ± 0.5
115	4.71 ± 0.04	87.3 ± 0.7
120	4.99 ± 0.03	92.4 ± 0.6
124	5.23 ± 0.04	96.9 ± 0.7

N.B.: the measurements were taken over several sessions, and the data sets were {120, 110, 100 G} using an aquisition time of 300 s; {90, 80, 70 G} with 300 s; {124, 115, 105, 95 G} with 180 s; and {85, 75 G} with 180 s. However, it was later determined the set {90, 80, and 70 G} yielded significant deviation from the trends in V_0 established by the others (e.g., a break in monotonicity for β). Because this was attributed to an error in the zeroing and placement of the gaussmeter, the data set was retaken. Recalculation using the new data set removed the deviation, so the data was replaced.

III.2. Measurements of Energy

To determine the electron kinetic energy for each B, we locate the peak of an MCA spectrum taken at V_0, and determine the energy K of the peak.

We obtain 10-minute acquisitions at each value of B, setting the velocity selector to V_0 as calculated from Section III.1 to obtain maximum signal. In general, the location of the peak is not strongly dependent on the (systematic) error in V_0, as long as the energy spectrum is acquired reasonably close (within ~ 0.1 kV) to V_0. Nevertheless, since we retook data for {70, 80, 90 G}, we decided to replace the corresponding data for the energy spectra as well. Thus, note that the data presented here use the retaken spectra.

To find the peaks, Kevin Galiano developed the algorithm of fitting the MCA spectra to the sum of a Lorentzian with a linear background. The specific fit function due to KG is

$$y = \frac{C_1 \cdot |\gamma| / \pi}{(x-n)^2 + \gamma^2} + C_2 x + C_3$$

where y is the number of counts in channel x. We are interested in n, which gives the peak of the spectrum, along with its fit error. The results are summarized in Table II below.

TABLE II. Determinations of channel number and K using a Lorentzian fit with a linear background. The values for K were calculated as $K = \alpha n + \varepsilon$, as given by Eq. 7.

B Field (G)	Channel No. n	Energy K (keV)
70	144.3 ± 1.0	317.3 ± 0.7
75	173.2 ± 1.0	380.9 ± 0.5
80	183.7 ± 1.0	403.8 ± 0.5
85	215.5 ± 1.1	473.9 ± 0.4
90	224.5 ± 1.1	493.7 ± 0.5
95	259.5 ± 1.2	570.7 ± 0.1
100	283.0 ± 1.2	622.2 ± 0.3
105	307.4 ± 1.3	675.9 ± 0.3
110	330.0 ± 1.3	725.8 ± 0.4
115	354.0 ± 1.4	778.6 ± 0.3
120	378.6 ± 1.5	832.7 ± 0.4
124	390.1 ± 1.5	857.8 ± 0.6

IV. ANALYSIS OF DATA AND ERRORS

IV.1. Momentum vs. Velocity and e/m

From Eq. 1 and 3, we have the classical and relativistic relations between p and v. Using Eq. 5 and 6,

$$\beta = \frac{E}{B} = \frac{e}{m}\left(\frac{\rho}{c^2}\right) B$$

classically, while relativistically,

$$\beta\gamma = \frac{E/B}{\sqrt{1-(E/B)^2}} = \frac{e}{m}\left(\frac{\rho}{c^2}\right) B.$$

Using the data in Table I, we plot β and $\gamma\beta$ against B in Fig. 3, along with their linear fits. We find the relativistic model fits with $\chi^2_{10} = 0.99$ (45%) and the classical model with $\chi^2_{10} = 2.29$ (1.1%).

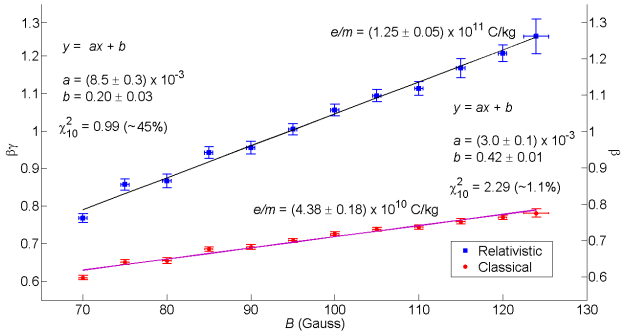

FIG. 3. Relativistic and classical linear fits of velocity vs. momentum data, from top to bottom. Note the dual axes, with relativistic on the left and classical on the right.

From the fit parameters, we can also extract an estimation of e/m using the slopes. Using $\rho = (20.3 \pm 0.2)$ cm for the radius of curvature, the relativistic model predicts $e/m = (1.25 \pm 0.05) \times 10^{11}$ C/kg, while the classical model predicts $e/m = (4.38 \pm 0.18) \times 10^{10}$ C/kg.

We note, however, that the above fit procedure yields y-intercept values which do not exist in either theories. The offsets are likely due to a systematic shift in our data, and to quantify the possible effects this might have on our results, we turn to a different analysis technique.

In Fig. 4, we plot the ratios $e/m = (\beta\gamma)/B \cdot c^2/\rho$ for the relativistic case, and $e/m = \beta/B \cdot c^2/\rho$ for the classical. This effectively eliminates the offset from consideration, and so is essentially equivalent to fitting $y = ax$.

The values of e/m that result are the error-weighted average of the trend.[4] For the relativistic case, we get $e/m = (1.562 \pm 0.008) \times 10^{11}$ C/kg, while for the classical case, we get $e/m = (1.062 \pm 0.003) \times 10^{11}$ C/kg.

Observing the χ^2 values from the first analysis method, as well as the trends in e/m in the second method, we conclude the relativistic model is more self-consistent than the classical one. We therefore decide to use the relativistic model to obtain a best estimate of e/m.

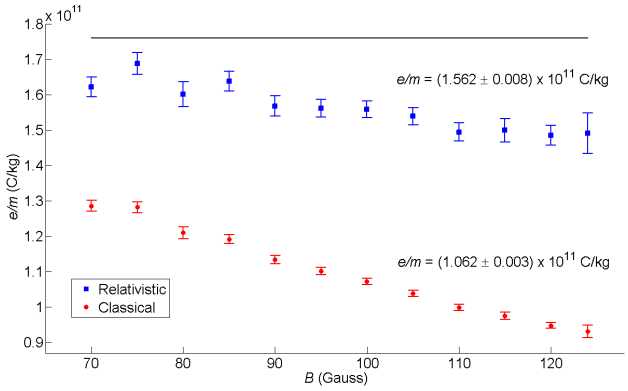

FIG. 4. Estimates of e/m for varying values of B. The relativistic case is on top and the classical below. For reference, the true value of e/m is plotted on top.

Taking the error-weighted average from the two approaches, we find $e/m = (1.554 \pm 0.008) \times 10^{11}$ C/kg. By considering the differences between the two methods, we arrive at an estimation of the lower bound on the systematic error on e/m of approximately 0.31×10^{11}C/kg.

IV.2. Velocity vs. Energy and mc^2

From Eq. 2 and 4, we have the classical and relativistic relations between K and v. Using Eq. 5 and 6, we have

$$K = \frac{1}{2}mc^2(E/B)^2 = \frac{1}{2}mc^2\beta^2$$

classically, and, in special relativity,

$$K = mc^2\left(1/\sqrt{1-(E/B)^2} - 1\right) = mc^2(\gamma - 1).$$

Using the data in Table II, we perform a linear fit to K against $\gamma - 1$ and β^2. (We do not show the plot here, but it is analogous to Fig. 3 from Section IV.1. See also KG's lab report for a plot of the inverted fit.)

Using the model $y = ax + b$, the fit parameters for the relativistic case are $a = 771 \pm 28$ and $b = -64 \pm 11$, with a $\chi^2_{10} = 0.60$ (82%). For the relativistic case, we get $a = 1077 \pm 39$ and -276 ± 20, with a $\chi^2_{10} = 1.93$ (3.7%).

From the fit parameters, we can also extract an estimation of mc^2 using the slopes. Hence, the relativistic model predicts $mc^2 = (771 \pm 28)$ keV, while the classical model predicts $mc^2 = (2150 \pm 76)$ keV.

Again, we note a systematic offset evident in the linear fits. We therefore take the same approach as in Section IV.1, and examine the trend of mc^2 for various B as predicted by the relativistic and classical models.

In Fig. 5, we plot the ratios $K/(\gamma-1)$ for the relativistic case and $2K/\beta^2$ for the classical. This effectively eliminates the offset from consideration, and so is essentially equivalent to fitting $y = ax$.

The values of mc^2 that result are the error-weighted average of the trend.[4] For the relativistic case, we get $mc^2 = (607 \pm 5)$ keV, while for the classical case, we get $e/m = (1016 \pm 5)$ keV.

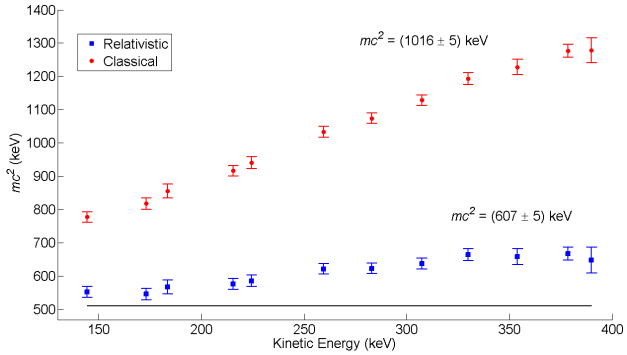

FIG. 5. Estimates of mc^2 for varying values of B. The classical case is on top and the relativistic below. For reference, the true value of mc^2 is plotted on the bottom.

Observing the χ^2 values from the first analysis method, as well as the trends in e/m in the second method, we conclude again that the relativistic model is more self-consistent than the classical one. Thus, we again use the relativistic model to obtain a best estimate of mc^2.

Taking the error-weighted average from the two approaches, we find $mc^2 = (612 \pm 5)$ keV. By considering the differences between the two methods, we arrive at an estimation of the lower bound on the systematic error on mc^2 of approximately 164 keV.

IV.3. Systematic Error

The systematic offset observed above was explored in terms of the possibility of a scaling factor for the B field measurements due to calibration error. It was found the ~ 0.1 kV shifts in V_0 values from predicted can be roughly explained by a factor of 0.95 (Note that at these fields, V_0 is essentially linear in B.)

Nevertheless, the final offset remains anomalous, since the effect is not simply a down-shift, but rather a non-linear rescaling of γ at high B fields, causing a "tilt" in the slope of the linear fits. This is readily seen in the slight but monotonic variations in the relativistic e/m estimates in Fig.4 and Fig.5. Determining the exact source of the systematic error remains difficult.

V. CONCLUSIONS

Comparing the classical and relativistic models, we find the former deviates significantly to χ^2 probabilities well below 10%. Fig. 4 and 5 show a strong, monotonic dependence of the classical predictions for e/m and mc^2 on the momentum of the electrons. The data strongly suggests special relativity is more self-consistent.

Using the relativistic model, we find the charge-to-mass ratio to be $e/m = (1.55 \pm 0.008_{\text{rand.}} \pm 0.31_{\text{syst.}}) \times 10^{11}$ C/kg and the electron mass to be $mc^2 = (612 \pm 5_{\text{rand.}} \pm 170_{\text{syst.}})$ keV. Compared to the established values of $e/m = 1.759 \times 10^{11}$ C/kg and $mc^2 = 511$ keV, these are errors of about 10% and 20%, respectively.

[1] R. Resnick, *Introduction to Special Relativity* (John Wiley & Sons, 1968).
[2] M.I.T. Junior Lab Staff, "Relativistic Dynamics: The Relations Among Energy, Momentum, and Velocity of Electrons and the Measurement of e/m," (2011).
[3] B. Crasemann, J. G. Pengra, and I. E. Lindstrom, Phys. Rev. **108**, 1500 (1957).
[4] P. R. Bevington and D. K. Robinson, *Data Reduction and Error Analysis for the Physical Sciences*, 3rd ed. (McGraw-Hill, 2003).

ACKNOWLEDGMENTS

EN gratefully acknowledges his lab partner, Kevin Galiano, and the Junior Lab staff for their assistance in understanding the theory behind the design and analysis of this experiment.